Journal of Applied Physics

High thermal stability and sluggish crystallization kinetics of high-entropy bulk metallic glasses

Cite as: J. Appl. Phys. **119**, 245112 (2016); https://doi.org/10.1063/1.4955060
Submitted: 08 March 2016 . Accepted: 18 June 2016 . Published Online: 30 June 2016

M. Yang, X. J. Liu, H. H. Ruan, Y. Wu, H. Wang, and Z. P. Lu

JOURNAL OF APPLIED PHYSICS **119**, 245112 (2016)

High thermal stability and sluggish crystallization kinetics of high-entropy bulk metallic glasses

M. Yang,[1,2] X. J. Liu,[1] H. H. Ruan,[2] Y. Wu,[1] H. Wang,[1] and Z. P. Lu[1,a)]
[1]*State Key Laboratory for Advance Metals and Materials, University of Science and Technology, Beijing 10083, People's Republic of China*
[2]*Department of Mechanical Engineering, The Hong Kong Polytechnic University, Hung Hom, Kowloon, Hong Kong*

(Received 8 March 2016; accepted 18 June 2016; published online 30 June 2016)

Metallic glasses are metastable and their thermal stability is critical for practical applications, particularly at elevated temperatures. The conventional bulk metallic glasses (BMGs), though exhibiting high glass-forming ability (GFA), crystallize quickly when being heated to a temperature higher than their glass transition temperature. This problem may potentially be alleviated due to the recent developments of high-entropy (or multi-principle-element) bulk metallic glasses (HE-BMGs). In this work, we demonstrate that typical HE-BMGs, i.e., ZrTiHfCuNiBe and ZrTiCuNiBe, have higher kinetic stability, as compared with the benchmark glass Vitreoy1 ($Zr_{41.2}Ti_{13.8}Cu_{12.5}Ni_{10}Be_{22.5}$) with a similar chemical composition. The measured activation energy for glass transition and crystallization of the HE-BMGs is nearly twice that of Vitreloy 1. Moreover, the sluggish crystallization region $\Delta T_{pl\text{-}pf}$, defined as the temperature span between the last exothermic crystallization peak temperature T_{pl} and the first crystallization exothermic peak temperature T_{pf}, of all the HE-BMGs is much wider than that of Vitreloy 1. In addition, high-resolution transmission electron microscopy characterization of the crystallized products at different temperatures and the continuous heating transformation diagram which is proposed to estimate the lifetime at any temperature below the melting point further confirm high thermal stability of the HE-BMGs. Surprisingly, all the HE-BMGs show a small fragility value, which contradicts with their low GFA, suggesting that the underlying diffusion mechanism in the liquid and the solid of HE-BMGs is different. *Published by AIP Publishing.*
[http://dx.doi.org/10.1063/1.4955060]

I. INTRODUCTION

High entropy alloys (HEAs) and bulk metallic glasses (BMGs) are both interesting metallic materials and attract extensive attention recently. HEAs tend to form simple solid solution structure such as face-centered cubic (FCC) or body-centered cubic (BCC), instead of intermetallic compounds[1] due to their high mixing entropy. It was reported that HEAs possess not only high recrystallization temperatures but also high recrystallization activation energy.[2] Tsai *et al*.[3] have also shown slow atomic diffusion and the related high activation energy, which originated from significant fluctuation of lattice potential energy[4] between lattice sites in HEAs. However, a high-entropy (HE) system sometimes could lead to formation of glassy structures, rather than concentrated solid solutions.[5] Such alloys were termed as high-entropy BMG (HE-BMG) which usually consists of at least five constituent elements with an equi-atomic or near equi-atomic ratio.[6] Actually, the first HE-BMG, ZrTiHfCuNi, was reported by Ma *et al*. in 2002,[7] and the maximum attainable diameter of 1.5 mm was fabricated. As HE-BMGs are a relatively new comer to the glass family, only a few HE-BMGs have been developed up to date; Zhao *et al*.[8] prepared the $Zn_{20}Ca_{20}Sr_{20}Yb_{20}(Mg_{0.55}Li_{0.45})_{20}$ MG with a rather low glass transition temperature of 50 °C while Ding *et al*.[9] demonstrated that the ZrTiHfCuNiBe HE-BMG with a critical diameter as large as 15 mm could be prepared. Recently, a few other HE-BMGs such as ZrTiCuNiBe,[10] PdPtCuNiP,[11] and ZrTiHfCuBe[12] were also reported.

Comparing with conventional BMGs, properties such as thermal stability and tardy crystallization process have not yet been systematically investigated for HE-BMGs, nevertheless, they are critical for future industrial applications. We have also noticed that most HE-BMGs were derived from existing BMGs; for example, the ZrTiCuNiBe and PdPtCuNiP HE-BMG were based on the benchmark glass Vitreloy 1[13] and $Pd_{40}Cu_{20}Ni_{20}P_{20}$[14] BMG, respectively. However, crystallization behavior of HE-BMGs upon reheating, as exemplified by multi-peaks in their differential scanning calorimeter (DSC) curve,[9] is totally different from that of the conventional BMGs in the same alloy system. The high-entropy effect may be able to impede nucleation and growth of crystalline phases due to the sluggish atomic diffusion, thus giving rise to high thermal stability. All above anomalies and conjecture encourage us to investigate crystallization behavior and the underlying mechanisms of HE-BMGs. In this study, therefore, we securitized the thermal stability and sluggish crystallization process of two typical HE-BMGs, i.e., ZrTiCuNiBe and ZrTiHfCuNiBe. For comparison, Vitreloy 1 was selected as the benchmark glassy alloy for our study.

a)Author to whom correspondence should be addressed. Electronic mail: luzp@ustb.edu.cn. Tel.: +86 10 82375387. Fax: +86 10 62333447.

II. EXPERIMENTAL

Ingots with a nominal composition of ZrTiCuNiBe,[10] ZrTiHfCuNiBe,[9] and $Zr_{41.2}Ti_{13.8}Cu_{12.5}Ni_{10}Be_{22.5}$ (i.e., Vitreloy 1)[13] were prepared by arc-melting under Ti-gettered high-purity argon atmosphere. The purity level of the constituent elements of Zr, Ti, Hf, Cu, Ni, and Be is 99.99, 99.99, 99.99, 99.99, 99.99, and 99.5 at. %, respectively. Each ingot was re-melted for at least six times for ensuring chemical homogeneity. BMG rods with a diameter of 3 mm and a length of about 30 mm were obtained by copper mold suction casting.

Amorphous nature of the as-cast rods was examined by X-ray diffraction (XRD) using Rigaku D/max-RB spectrometry with Cu K α radiation ($\lambda = 0.15406$ nm). Thermal properties were characterized using a NETZSCH DSC 404 F1 Pegasus® differential scanning calorimeter (DSC) with protection of argon at a flow rate of 60 ml/min and heating rates ranging from 5 to 40 K/min. The DSC system was calibrated using the indium and zinc standards. In order to identify crystalline phases, high-resolution transmission electron microscopy (HRTEM) JEM-2010 was employed. TEM samples were first mechanically ground into 40 μm in thickness, followed by ion milling in liquid nitrogen.

III. RESULTS

DSC traces of the ZrTiCuNiBe and ZrTiHfCuNiBe HE-BMGs, hereafter denoted as H1 and H2, at the heating rates of 5, 10, 20, 30, and 40 K/min are shown in Fig. 1. The result of Vitreloy 1 (denoted as V1 hereafter) is also included for comparison. Glass transition temperature, T_g, onset crystallization temperature T_x, peak temperature of the first exothermic crystallization event T_{pf} and the last exothermic reaction T_{pl}, melting temperature T_m and liquid temperature T_l are compiled in Table I. The definition of all these temperatures is indicated clearly by arrows in Fig. 1. The supercooled region, $\Delta T_{x\text{-}g}$ and the crystallization region, $\Delta T_{pl\text{-}pf}$, defined as the temperature range between T_{pl} and T_{pf}, along with the reduced glass transition temperature T_{rg} that given by T_g/T_l,[15] the glass-forming ability (GFA) parameter γ defined as $T_x/(T_g + T_l)$[16–18] and the critical diameter for glass formation of V1, H1, and H2, are also listed in Table I. Apparently, the $\Delta T_{pl\text{-}pf}$ value reflects how wide the temperature range from the start to the completion of crystallization is. Fig. 2 shows dependence of T_g, T_x, T_m, $\Delta T_{x\text{-}g}$, and $\Delta T_{pl\text{-}pf}$ on alloy composition. Compared with that of the conventional BMG V1, T_g is increased about 50 K in the two HE-BMGs. Although all BMGs exhibited multiple exothermic crystallization peaks on their heating DSC traces, T_x of the two HE-BMGs is raised up approximately 40 K. These observations suggest that the HE-BMGs have a larger crystallization resistance during reheating than the conventional BMG in the same alloy system. Nevertheless, the supercooled region $\Delta T_{x\text{-}g}$ is decreased slightly, implying that the stability of HE-BMGs at the supercooled liquid state was not enhanced. Interestingly, the crystallization region $\Delta T_{pl\text{-}pf}$ is increased from 65 K of V1 to 111 and 217 K of H1 and H2, respectively. In particular, the peak temperature of the last crystallization reaction in H2 is close to the onset melting point T_m, indicating

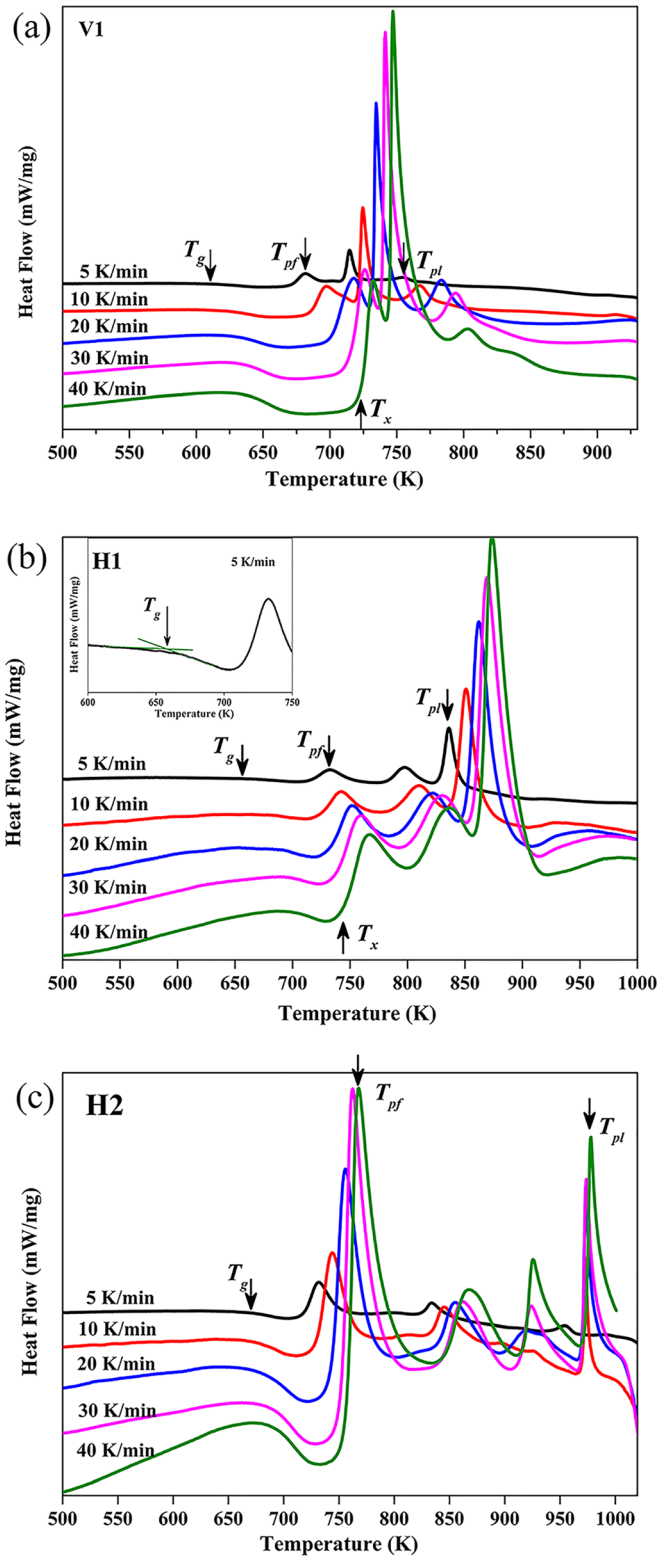

FIG. 1. DSC curves of (a) V1, (b) H1, and (c) H2 metallic glasses obtained at different heating rates.

that the entire crystallization process in the HE-BMGs was significantly prolonged and became really sluggish.

Based on the DSC data, the apparent activation energy can be calculated by the Kissinger model[19]

$$\ln\left(\frac{\beta}{T^2}\right) = -\frac{E(T)}{RT} + \text{constant}, \tag{1}$$

TABLE I. Characteristic temperatures of V1, H1, and H2 metallic glasses, along with the onset crystallization activation energy E_x, critical diameter d_c (mm), and GFA parameters T_{rg} and γ (heating rate: 20 K/min).

Alloys	T_g	T_x	$\Delta T_{x\text{-}g}$	T_{pf}	T_{pl}	T_m	T_l	$\Delta T_{pl\text{-}pf}$	E_{pf} (kJ/mol)	T_{rg} [T_g/T_l]	γ [$T_x/(T_g+T_l)$]	d_c
V1	628	701	73	718	783	940	1001	65	164.7 ± 6.7	0.627	0.430	>20[22]
H1	691	732	41	751	862	1077	1196	111	281.2 ± 16.1	0.578	0.388	3[10]
H2	681	743	62	756	973	1015	1168	217	237.7 ± 12.5	0.583	0.402	15[9]

where β is the heating rate, E(T) is the activation energy for glass transition or crystallization, T is the temperature, and R is the gas constant. The activation energy can be determined by using a plot of $\ln(\beta/T^2)$ versus 1/T for those BMGs, and the slope of which is $-E(T)/R$. As an example, Fig. 3 shows the variation of $\ln(\beta/T_{pf}{}^2)$ versus $1/T_{pf}$ for V1, H1, and H2. The data are well fitted by straight lines, implying that the crystallization behavior of both HE-BMGs and the conventional BMG V1 obey the above mentioned equation. The activation energy for crystallization was then estimated by evaluating the slope of these straight lines, and the obtained values of $E(T_{pf})$ for the three glasses are listed in Table I. It can be noticed that both the activation energies of the HE-BMGs are much higher than those of V1, further confirming the large thermal stability of the HE-BMGs against crystallization upon reheating.

In order to further compare the thermal stability of these BMGs, continuous heating transformation diagrams (i.e., lifetime prediction diagram) were constructed based on the method proposed previously.[20] For a given temperature T_{pf}, the corresponding β, which brings about crystallization, could be estimated[20]

$$\beta = T_{pf}{}^2 \exp(b/T_{pf} + c). \quad (2)$$

The heating time t_h from room temperature (i.e., 298 K) to T_{pf} can be obtained as

$$t_h = (T_{pf} - 298)/\beta. \quad (3)$$

Continuous heating transformation diagrams for T_{pf} versus t_h calculated from primary devitrification process are shown in Fig. 4, where the t_h is denoted in the logarithmic scale. The solid curves depict the T_{pf}-t_h relations for different glassy materials, whereas the dashed curves are the heating profiles in DSC experiments. The intersections between the dashed and solid curves are experimental data points extracted from the first exothermic peaks. After extrapolation of the solid curves, it is estimated that H1 and H2 remain stable at room temperature for more than 10^{20} years, which is much longer than that of V1 with merely 10^9 years. At 400 K, the lifetime of H1 and H2 is nearly 10^{11} years, which remains much more stable than V1 with 10^4 years.

IV. DISCUSSION

A. High thermal stability and sluggish crystallization of HE-BMGs

In multicomponent HEAs, atomic size difference, different bonding energy, and crystallographic structure among the constituent elements result the heavily lattice distortion in neighboring atoms sluggish atomic diffusion,[1,21] which could effectively inhibit phase transformation, as confirmed by the recent experimental findings that HEAs usually possess higher recrystallization temperatures and activation energies[2] than conventional alloys. Based on our earlier

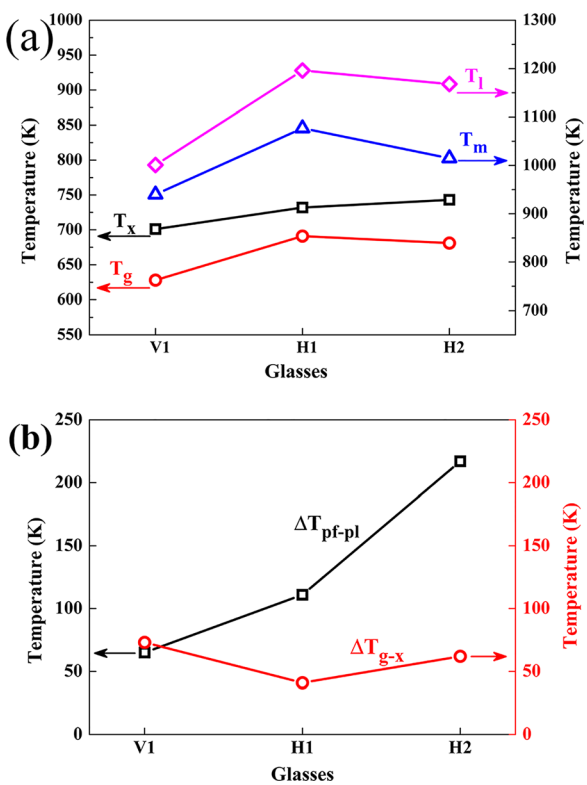

FIG. 2. Characteristic temperatures of the HE-BMGs. (a) T_g, T_x, T_m, and T_l; (b) $\Delta T_{g\text{-}x}$ and $\Delta T_{pl\text{-}pf}$.

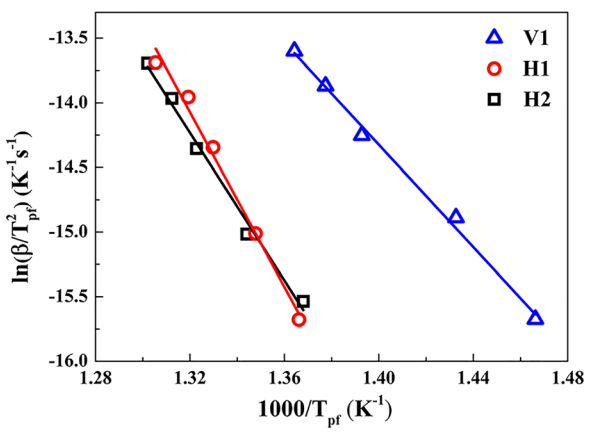

FIG. 3. Kissinger plot of the onset crystallization temperature T_x for V1, H1, and H2 metallic glasses. Activation energy was derived from the slop of these curves.

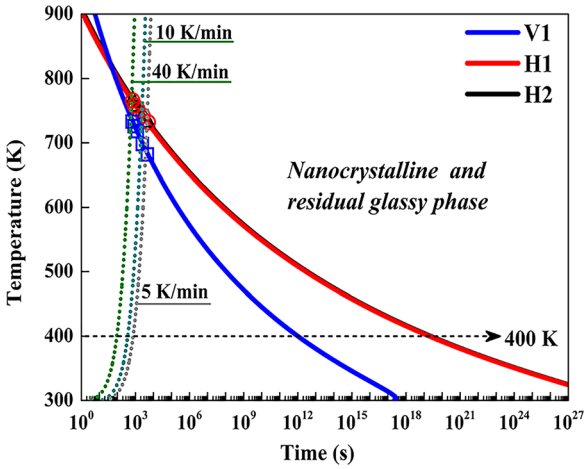

FIG. 4. Continuous heating transformation diagrams of primary precipitation for V1, H1, and H2. The dashed vertical line indicates the heating curves at a rate of 5–40 K/min.

results shown in Figs. 1 and 3, it was suggested that the HE-BMGs seemingly have larger thermal stability against crystallization upon reheating, as compared with the conventional BMGs in the same alloy system. In order to verify the slow crystallization process conceived based on the DSC results, XRD and TEM experiments were carried out on the V1 and H1 samples. H1 and V1 have the same elemental species, and both exhibited three separate exothermic peaks, which facilitates easy comparison between them. For each BMG, we have selected three temperatures for study, i.e., the end temperature of the first, second, and last exothermal peaks on the DSC curves, denoted as T_1, T_2, and T_3, respectively. Note that the annealing temperatures T_1, T_2, and T_3 of H1 are 799, 865, and 922 K, respectively, much higher than the corresponding temperature of V1, i.e., $T_1 = 741$ K, $T_2 = 787$ K, and $T_3 = 834$ K. All the specimens were first continuously heated at a rate of 40 K/min to a preset temperature and immediately cooled. Although the crystallization cannot be avoided, the information regarding average size, nucleation, and growth kinetics of crystallinities and transformation fraction of the amorphous matrix can reflect the crystallization resistance during heating.

XRD patterns of all the specimens heat-treated to different temperatures are shown in Fig. 5, and the corresponding TEM images are shown in Figs. 6 and 7. Based on the XRD results, it is clear that the crystallization products in H1 and V1 are different, although both of them showed three exothermic peaks on their DSC trace. At T_1, H1 shows a broad halo superimposed with a few crystalline peaks on its XRD pattern, indicating that this specimen still consists of a large portion of amorphous structure. The primary phase was identified as FCC (face-centered cubic), but changed to the intermetallic compound Zr_2Cu in V1. Although the actual annealing temperature T_1 for H1 (i.e., 799 K) is higher than that of V1 (i.e., 741 K), it seems that the percentage of the amorphous matrix remained in H1 after the first annealing is still higher than that in V1, confirming a much retarded crystallization process in the HE-BMG, consistent with the earlier DSC results. From the TEM images shown in Fig. 6, it is confirmed that nanocrystal grains with different

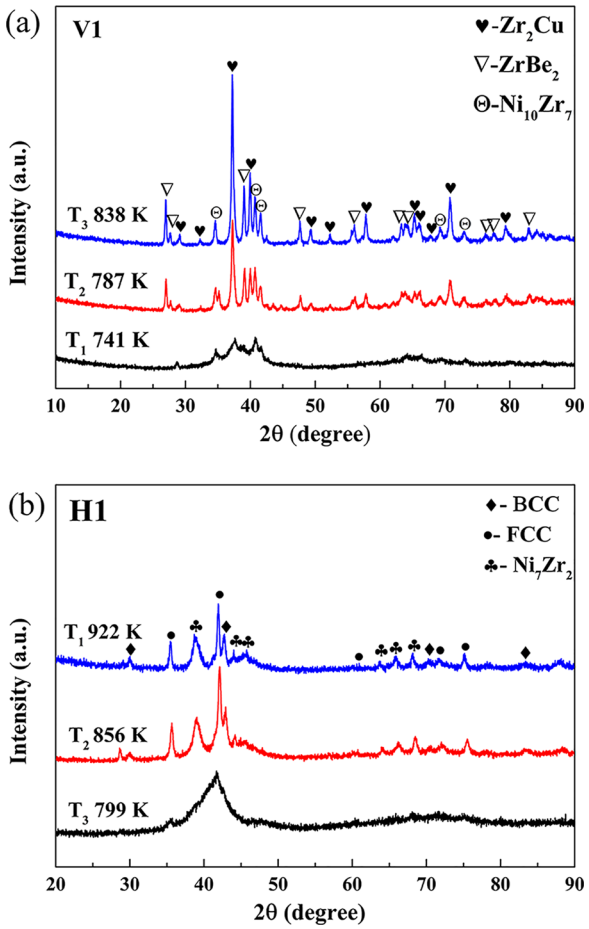

FIG. 5. XRD patterns of (a) V1 and (b) H1 glasses annealed at different temperatures.

crystallographic structures were precipitated in both kinds of BMGs. Nevertheless, their corresponding dark field images ambitiously reveal that the FCC nanoparticles in H1 have a smaller volume fraction (i.e., a high fraction of amorphous matrix remained) and size, as compared with those of the Zr_2Cu phase in V1, further verifying a larger crystallization resistance of the HE-BMG.

As the annealing temperature increased, i.e., T_2 and T_3, a new BCC (body-centered cubic) phase and eventually the Ni_7Zr_2 compound gradually appeared in the HE-BMG matrix while two additional intermetallic compounds, i.e., $ZrBe_2$ and $Ni_{10}Zr_7$, were formed in V1 based on the XRD measurements shown in Fig. 5 and the selected area diffraction patterns in Fig. 7. From Fig. 7, it is seen that the average grain size of all the crystallinities in H1 is appreciably smaller than that in V1, although the actual annealing temperature for H1 is much higher. All above results indicate that high mixing entropy can successfully retard lattice diffusion during reheating, and consequently, enhance the thermal stability of HE-BMGs.

B. Dilemma between thermal stability and GFA

While the above results have indicated that HE-BMGs have higher thermal stability against crystallization than conventional BMGs with the same constituents, the significant difference in their GFA should be stressed. The GFA of V1,

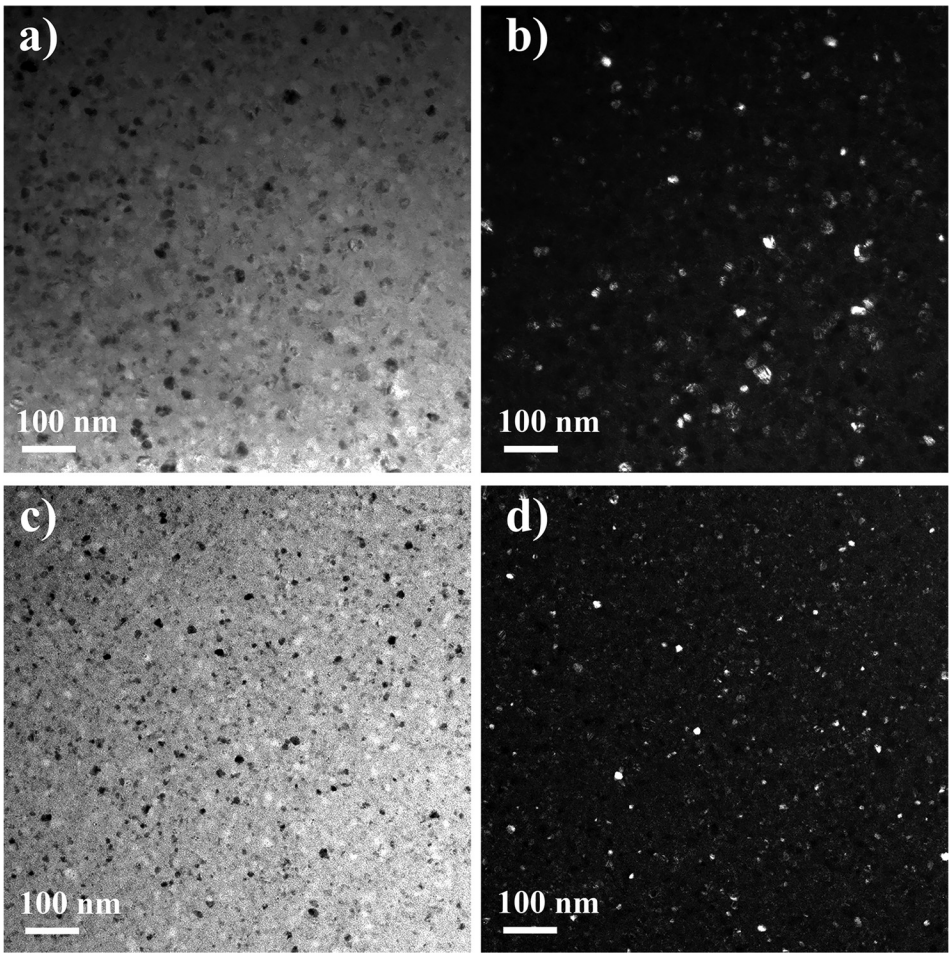

FIG. 6. TEM images of V1 and H1 glasses annealed at 741 and 799 K, respectively; (a) bright-field image of V1, (b) dark-field image of V1, (c) bright-field image of H1, and (d) dark-field image of H1.

in terms of the attainable maximum diameter, is above 20 mm.[22] However, the GFA of H1 and H2 was dramatically reduced (see Table I). Considering the higher thermal stability of the HE-BMGs upon reheating, the fundamental question here is why the thermal stability is not in line with the GFA if both are referred to the ability of retarding crystallization. In literature, fragility is a measure of the sensitivity of the atomic rearrangement rate to temperature,[23–25] which can therefore be regarded as an indicator of GFA. Accroding to the change of viscosity η with the scaled temperature T_g/T, Angell[26] introduced the classification of strong and fragile liquids. In general, a strong liquid (for example, silica) can be vitrified under a slow cooling rate since the logarithmic magnitude of viscosity or relaxation time increases linearly with temperature. The fragile liquid, however, must be vitrified by applying a fast cooling rate since its logarithmic viscosity only increases precipitously within a very narrow temperature window near its T_g.[27] The fragility m was then defined to be the slope of Angell's plot at T_g, which is given by[27,28]

$$m = \frac{DT_0T_g}{(T_g - T_0)^2 ln10}, \tag{4}$$

where D is the strength parameter in the Vogel–Fulcher–Tammann (VFT) equation, which controls how closely the liquid system obeys the Arrhenius law. T_0 is the asymptotic value of T_g, which is usually approximated as the onset of the glass transition temperature at the limit of infinitely slow cooling, and T_g is the glass transition temperature at a heating rate of 20 K/min. The variation of T_g with the heating rate β can be fitted by using the Vogel–Fulcher–Tammann (VFT) equation[29]

$$\ln\beta = \ln\beta_0 - DT_0/(T_g - T_0), \tag{5}$$

where β_0 is a constant, T_0 and D can be obtained by fitting the VFT equation from the heating rate dependence of T_g, then the fragility index m can be calculated using Eq. (4). Figure 8 shows the variation of $\ln\beta$ with T_g fitted by VFT equation for the HE-BMGs and V1. The m value of H1 and H2 is calculated to be 20.1, and 21.2, which is much smaller than that of V1 ($m = 40$) in the same alloy system. The m value obtained in this study for H1 and V1 is similar with the results reported by Gong *et al.*,[30] i.e., $m = 23$ for H1 and $m = 44$ for V1. For strong liquids,[31] $m < 30$ with a lower limit of ~16. For example, strong glass formers like SiO_2 and GeO_2 have $m = 20$ at T_g.[32] Fragile liquids, on the other hand, are associated with $m > 100$. In this sense, the studied HE-BMGs can be classified to the strong glass former, which is obviously in contrast with their actual GFA.

In general, metallic glasses which process high crystallization activation energy, sluggish crystallization process in heating process, and a small fragility m value are probably good glass formers. Based on our above results, the GFA of the HE-BMGs H1 and H2 cannot be directly represented by

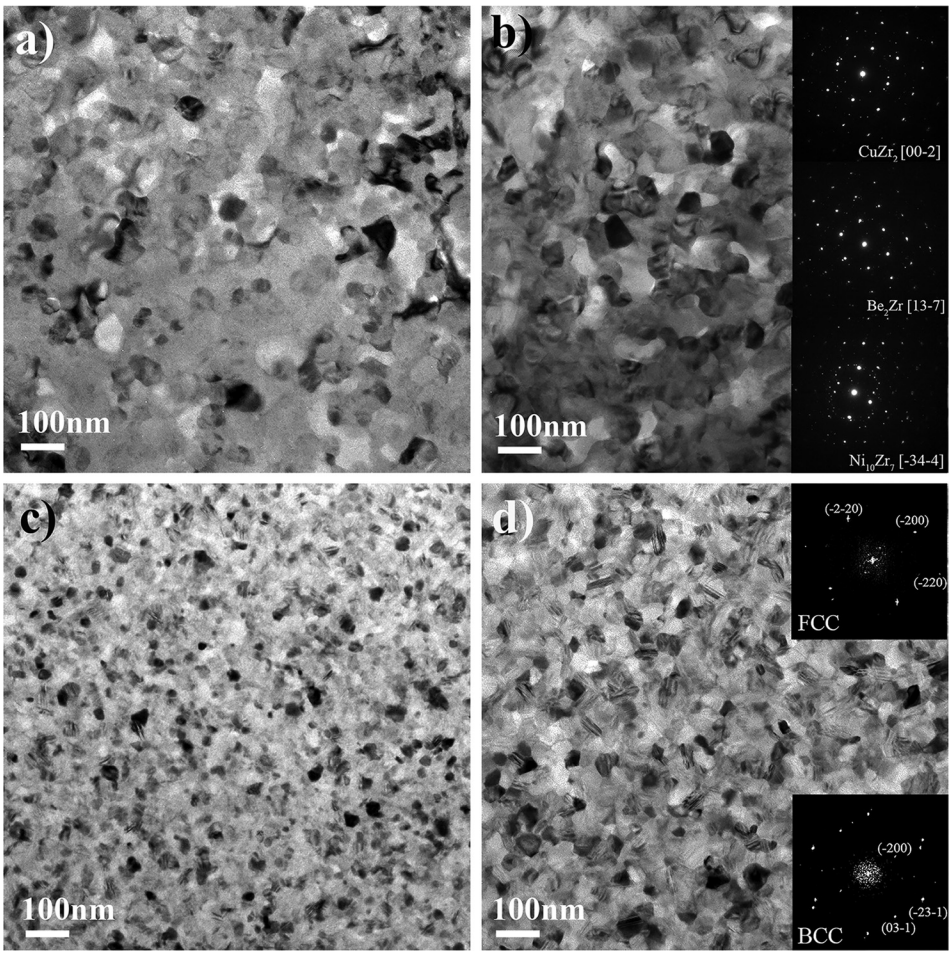

FIG. 7. TEM images of V1 and H1 glasses annealed at different temperatures; (a) V1, 787 K, (b) V1, 834 K, (c) H1, 856 K, and (d) H1, 922 K.

their m values. This dilemma might be related to the breakdown of the Stoke-Einstein equation at low temperatures,[33–36] indicating that the diffusivity and viscosity are no longer related when the melt is vitrified. GFA is mainly governed by the variation of viscosity with temperature at the undercooled liquid state, whilst crystallization upon reheating is mediated by atomic diffusion in solid matrix. According to Adam–Gibbs equation,[37] the high entropy of mixing can lead to low viscosity and a high mobility of the atoms in the liquid, which would accelerate crystallization during cooling, and decreasing the GFA. HE-BMGs may not be cast into large sizes but can well retard crystallization once it is vitrified because of small diffusivity in solid matrix. In other words, applicability of the fragility parameter to reflect GFA of HE-BMGs needs to be carefully verified. Actual underlying mechanisms of the inverse relationship between the thermal stability and GFA in HE-BMGs are still unclear, which merits further investigation.

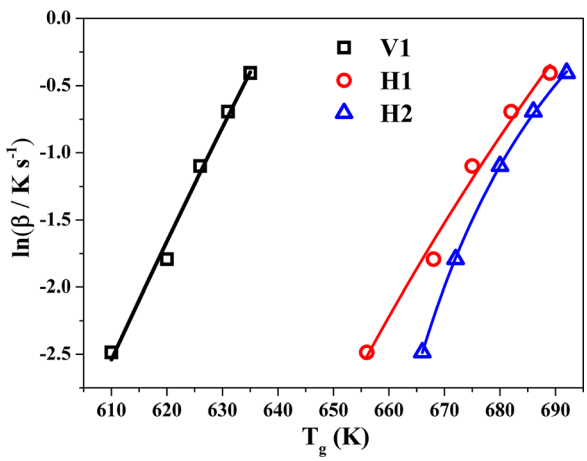

FIG. 8. The VFT relationship between T_g and lnβ for V1 and the HE-BMGs.

V. CONCLUSIONS

We have systematically investigated thermal stability and crystallization behavior of two HE-BMGs, in comparison with those of a representative conventional glass Vitreloy 1 in the same alloy system. Main results can be summarized as follows:

(1) The HE-BMGs have shown an increased glass transition temperature and onset crystallization temperature. The apparent activation energy for glass transition and crystallization estimated by Kissinger plot dramatically increased. All these observations indicate that the HE-BMGs have much larger thermal stability upon reheating than the conventional BMG with the same constituents, and high-entropy configuration state can effectively retard relaxation and crystallization kinetics.
(2) The crystallization region, i.e., the span between the onset and end crystallization temperature, was greatly increased in the HE-BMGs. In addition, the continuous heating

transformation diagram suggested that HE-BMGs possess much longer lifetime at room temperature. Moreover, detailed TEM characterization demonstrated and confirmed that nucleation and grain growth of crystallinities in the HE-BMG matrices are much slower than in conventional BMGs. All these results suggest that high mixing entropy which retards atomic lattice diffusion can lead to a sluggish crystallization process.

(3) The fragility parameter m of the HE-BMGs can be classified to strong glasses, which is in contrast to their low GFA. This dilemma is related to the breakdown of the Stoke-Einstein equation at low temperatures and the fact that the diffusion at the liquid and solid state is determined by different mechanisms.

ACKNOWLEDGMENTS

This research was supported by the National Natural Science Foundation of China (Nos. 51531001, 51422101, 51271212, and 51371003), 111 Project (B07003), International S&T Cooperation Program of China (2015DFG52600) and Program for Changjiang Scholars and Innovative Research Team in University (IRT_14R05), Fundamental Research Fund for the Central Universities (Nos. FRF-TP-15-004C1 and FRF-TP-14-009C1). Y.W. was supported by Beijing Youth Talent Plan (YETP0408) and "Beijing Higher Education Young Elite Teacher Project," and X.J.L. acknowledges the financial support from the Program for New Century Excellent Talents in University (NCET-13-0663).

[1]J. W. Yeh, S. K. Chen, S. J. Lin, J. Y. Gan, T. S. Chin, T. T. Shun, C. H. Tsau, and S. Y. Chang, Adv. Eng. Mater. **6**, 299 (2004).
[2]J. W. Yeh, Ann. Chim. - Sci. Mater. **31**, 633 (2006).
[3]K. Y. Tsai, M. H. Tsai, and J.-W. Yeh, Acta Mater. **61**, 4887 (2013).
[4]G. H. Vineyard, Phys. Rev. **102**, 981 (1956).
[5]S. Guo, Q. Hu, C. Ng, and C. T. Liu, Intermetallics **41**, 96 (2013).
[6]W. H. Wang, JOM **66**, 2067 (2014).
[7]L. Ma, L. Wang, T. Zhang, and A. Inoue, Mater. Trans. **43**, 277 (2002).
[8]K. Zhao, X. X. Xia, H. Y. Bai, D. Q. Zhao, and W. H. Wang, Appl. Phys. Lett. **98**, 141913 (2011).
[9]H. Y. Ding, Y. Shao, P. Gong, J. F. Li, and K. F. Yao, Mater. Lett. **125**, 151 (2014).
[10]H. Y. Ding and K. F. Yao, J. Non-Cryst. Solids **364**, 9 (2013).
[11]A. Takeuchi, N. Chen, T. Wada, Y. Yokoyama, H. Kato, A. Inoue, and J. W. Yeh, Intermetallics **19**, 1546 (2011).
[12]S. F. Zhao, G. N. Yang, H. Y. Ding, and K. F. Yao, Intermetallics **61**, 47 (2015).
[13]A. Peker and W. L. Johnson, Appl. Phys. Lett. **63**, 2342 (1993).
[14]A. Inoue and N. Nishiyama, Mater. Sci. Eng., A **226–228**, 401 (1997).
[15]D. Turnbull, Contemp. Phys. **10**, 473 (1969).
[16]Z. Lu and C. Liu, Acta Mater. **50**, 3501 (2002).
[17]Z. Lu, Y. Liu, and C. T. Liu, *Bulk Metallic Glasses* (Springer, 2008), p. 87.
[18]Z. Lu and C. Liu, Phys. Rev. Lett. **91**, 115505 (2003).
[19]H. E. Kissinger, Anal. Chem. **29**, 1702 (1957).
[20]D. V. Louzguine and A. Inoue, Appl. Phys. Lett. **81**, 2561 (2002).
[21]T. K. Chen, T. T. Shun, J. W. Yeh, and M. S. Wong, Surf. Coat. Technol. **188**, 193 (2004).
[22]W. L. Johnson, in *Fundamental Aspects of Bulk Metallic Glass Formation in Multicomponent Alloys* (Trans Tech Publ, 1996), p. 35.
[23]C. T. Moynihan and S. Cantor, J. Chem. Phys. **48**, 115 (1968).
[24]M. Tatsumisago, B. Halfpap, J. Green, S. Lindsay, and C. Angell, Phys. Rev. Lett. **64**, 1549 (1990).
[25]C. Angell, J. Non-Cryst. Solids **73**, 1 (1985).
[26]C. Angell, J. Non-Cryst. Solids **131**, 13 (1991).
[27]C. A. Angell, Science **267**, 1924 (1995).
[28]R. Böhmer and C. A. Angell, Phys. Rev. B **45**, 10091 (1992).
[29]R. Brüning and K. Samwer, Phys. Rev. B **46**, 11318 (1992).
[30]P. Gong, S. Zhao, H. Ding, K. Yao, and X. Wang, J. Mater. Res. **30**, 2772 (2015).
[31]D. Perera, J. Phys.: Condens. Matter **11**, 3807 (1999).
[32]J. C. Mauro, Y. Yue, A. J. Ellison, P. K. Gupta, and D. C. Allan, Proc. Natl. Acad. Sci. U.S.A. **106**, 19780 (2009).
[33]M. T. Cicerone and M. Ediger, J. Phys. Chem. **97**, 10489 (1993).
[34]F. Fujara, B. Geil, H. Sillescu, and G. Fleischer, Z. Phys. B: Condens. Matter **88**, 195 (1992).
[35]N. Lazarev, A. Bakai, and C. Abromeit, J. Non-Cryst. Solids **353**, 3332 (2007).
[36]G. Tarjus and D. Kivelson, J. Chem. Phys. **103**, 3071 (1995).
[37]G. Adam and J. H. Gibbs, J. Chem. Phys. **43**, 139 (1965).